Moroccan Journal of Chemistry
ISSN: 2351-812X
http://revues.imist.ma/?journal=morjchem&page=login
Mahardiani & al. / Mor. J. Chem. 10 N°2 (2022) 337-350
DOI: https://doi.org/10.48317/IMIST.PRSM/morjchem-v10i2.32648

Nanofiber Fabrication from Palm Fiber Waste for Sustainable Water Remediation

Lina Mahardiani[a]*, Pingki Wahyu Septianing[a], Pundung Setia Lesana[a], Sulistyo Saputro[a], and Sunu Pranolo[b]

[a]*Chemistry Education Study Program, Faculty of Teacher Training and Education, Universitas Sebelas Maret, Surakarta*
[b]*Department of Chemical Engineering, Faculty of Engineering, Universitas Sebelas Maret, Surakarta*
Jl. Ir. Sutami 36A, Jebres, Kentingan, Surakarta, Indonesia

** Corresponding author:*
mahardiani.lina@staff.uns.ac.id
Received 27 April 2022,
Revised 12 May 2022,
Accepted 26 May 2022

Abstract

Palm fiber has the potential to be synthesized into nanofiber because it contains high enough cellulose, about 40-60%. The synthesis of nanofibers was carried out by chemo-mechanical methods. Chemical processes included delignification by alkali, acid hydrolysis, and bleaching. Meanwhile, the mechanical process consisted of grinding. Modifications were also made to the formed nanofibers, namely nano oxide coating. This study aimed to determine (1) the synthesis of nanofiber materials with palm fiber waste as adsorbent, (2) the crystallinity of the nanofiber structure, (3) the adsorption capacity of nanofiber adsorbents against congo red and methylene blue. FTIR characterization showed that the nanofiber material had been successfully synthesized, marked by specific peaks indicating the cellulose-forming functional group, namely -OH group at the peak of 3415.12 cm^{-1}, -CH group at the peak of 2897.21 cm^{-1}, -CO group at the peak of 1635.71 cm^{-1}, and -CH_2 at peak 1431.24 cm^{-1}. The crystallinity of the nanofibers reached 74.933% based on XRD results. Besides, this nanofiber had high adsorption power for cationic dyes (methylene blue) and lower adsorption power for anionic dyes (congo red). The maximum adsorption capacity (mg/g) of Nf HCl, Nf HCl + Fe 3%, Nf HCl + Fe 5% with contact temperatures of 30°C, 40°C, 50°C to methylene blue was 9.973; 9.959; 9.539; 9.924; 9.904; 9.698; 9.952; 9.931; 9.636; respectively. Meanwhile, the maximum adsorption capacity (mg/g) of Nf HCl, Nf HCl + Fe 3%, Nf HCl + Fe 5% with temperatures of 30°C, 40°C, 50°C against congo red respectively was 8.579; 9.421; 9.711; 8.184; 8.921; 9; 8.947; 8.342; 7.263. This results will be beneficial as a strategy to utilize the palm fiber waste for dyes removal from the aquatic ecosystem.

Keywords: *palm fiber, nanofiber, adsorption, congo red, methylene blue*

1. Introduction

Today, there are many environmental pollution cases. Environmental pollution is the entry or inclusion of living things, substances, energy, and/or other components into the environment by human activities so that they exceed the established environmental quality standards [1]. Pollution can occur on land, air, or water. Pollution of water areas can be sourced from industrial waste, agricultural waste, household waste, and others. Polluted water bodies are characterized by changes in color, changes in pH, gas generation, high organic matter content, low dissolved oxygen levels, and the death of animals in these waters [2]. One example of water pollution occurs in the Bengawan Solo River. According to research conducted by Roosmini et al. [3], the Bengawan Solo River has been polluted from upstream. This condition was related to industrial and domestic activities in the upstream watershed. The upstream Bengawan Solo River was classified as lightly and moderately polluted, with the most standard river parameters being Total Suspended Solid (TSS) and the least being Total Dissolve Solid (TDS). In addition, the poor status of water quality in this river was indicated by the parameters of biological oxygen demand (BOD), total phosphate, oil, and fat, which still exceed the quality standard. Pollutants originating from domestic waste, industrial waste, and agricultural waste contained organic, inorganic, and other components. The amount of this pollutant load was not proportional to the natural purification process, resulting in an oxygen deficit and a decrease in water quality [4]. In addition, the relatively common water pollutant comes from textile industry waste. Textile waste produced has the potential to pollute the environment because dyes dominate it with high concentrations and various chemical compounds [5]. The dyes generally used up to 80% of the processing process in the textile industry are azo dyes (Zolinger et al., 1987 in Sudha) [6]. Azo dyes are still used in the textile and paper industry due to their low cost and easy use [7]. In fact, azo dyes are classified as wastes difficult to decompose (degraded) and are toxic and carcinogenic at certain levels [8]. One type of this azo dye is congo red and methylene blue. Congo red and methylene blue dyes generally consist of azo compounds and their derivatives in the form of a benzene group. Azo compounds have the general structure R-N=N-R', where R and R' are the same or different organic chains. This compound has a -N=N- group, which is called the azo structure [9]. Congo red is also one type of anionic dye. Congo red is synthesized by combining bis-diazotized benzidine with two naphthenic acid molecules, salted using sodium chloride to form a red disodium salt [10].

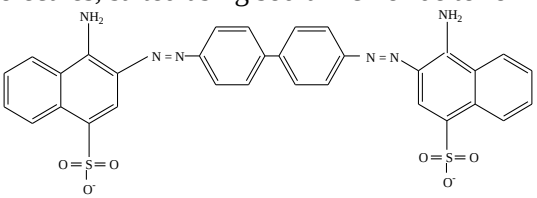

Figure 1. Congo Red Structure

Congo red (CR) is an azo dye [1-napthalenesulfonic acid, 3,3′-(4,4′-biphenylene bis(azo)) bis (4-amino-) disodium salt] in asymmetric form, included in azo sulfonate dye, and entered into a dye that can bind proteins. The presence of CR in a free environment can disrupt aquatic ecosystems, especially for aquatic plants and fish, because it blocks light from entering the water. CR is also a dangerous and toxic dye because it can cause kidney cancer, liver cancer, and bladder cancer. Direct contact with the eyes can also cause allergies, skin irritation, respiratory system, and mucous membranes [7]. Meanwhile, methylene blue (MB) is one type of cationic dye, often used as a basic dye [11]. Methylene blue is a sulfur-containing and toxic aromatic heterocyclic compound with very strong adsorption capacity and is commonly used as a dye for silk, wool, paper, and cosmetics. This compound is a dark green crystal. When dissolved in water or alcohol, it produces a blue-colored solution. Methylene blue has a molecular weight of 319.86 g/mol, a melting point of 105°C, and a solubility of 4.36 x 10^4 mg/L [12-15]. This dye is difficult to decompose, stable

against chemical reactions, and toxic [16]. Furthermore, if the MB level in the water is too high, it can cause adverse effects on the environment and health if the water is consumed. The effects of methylene blue on health include irritation, nausea, vomiting, burns, anemia, and hypertension [15,17].

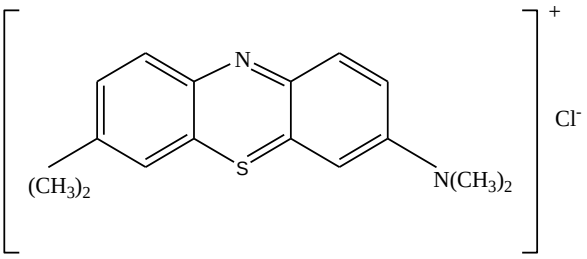

Figure 2. Methylene Blue Structure

In the regulation of the Minister of the Environment, the threshold for congo red and methylene blue dyes has been set at 5 mg/L [18]. On the other hand, several methods can be used to overcome dye pollutant, including chemical precipitation, ion exchange, membrane separation, electrolysis, extraction, and adsorption. Specifically, the adsorption process is quite effective for removing dye from wastewater [19]. This adsorption is a substance absorption on the solid surface. The advantages of the adsorption method are low cost, high efficiency in aqueous solutions, minimization of sludge formation, and ease of regeneration process [20]. In the adsorption process, an adsorbent is required. An adsorbent is a solid substance that absorbs specific components of a fluid phase. One of the adsorbent materials that can be used is nanofiber from palm fiber, in addition to activated carbon [21], zeolite [22], hydrotalcite [23]. In this regard, the palm tree is one of the multifunctional plants because almost all the physical and production parts of the palm tree can be utilized and have economic value. Usually, palm trees are used as fuel and building materials by taking a little of the outer bark. Along with the technological development, people can now use the palm stems in the pith to make flour [24].

Aren or palm sugar (*Arengga pinata*) is also a plant that produces industrial materials. There are five main products produced by palm trees: brown sugar, *kolang-kaling*, house roofs, water infiltration filters, and raw materials for making flour. Palm flour is obtained from starch extracted from mature palm tree trunks. Palm tree trunks contain 26-37% starch. In addition, the palm flour produced has a low protein and fat content so that it can be used as a food ingredient [25]. Moreover, the inner palm stem is usually ground to extract the starch and is commonly used to make vermicelli. The production process of palm stem milling produces liquid and solid waste. Solid waste in the form of bark and dregs in the form of fibers leftover from palm flour juice [26]. The dregs in the form of palm fiber are almost not used at all and are left to rot or dry out and then burned [27]. In comparison, the remaining milled fibers can be utilized to make nanofibers as an advanced adsorbent material. Nanofiber (Nf) has a long structure, large surface area, high porosity, and an interconnected pore structure. On the other hand, iron oxide (Fe_3O_4) has a large adsorption capacity, abundant presence, and is friendly to the environment [28]. Modification of nanofiber with iron oxide (Fe_3O_4) makes it stronger physically [29] and increases its adsorption capacity, making it suitable for treating water pollution by dyes [28]. Therefore, this study aimed to determine the nanofibers' characteristics synthesized from palm fiber waste, modified by nano-sized oxides as dye adsorbents, such as congo red and methylene blue.

2. Experimental

2.1. Chemical and Materials

The material used in this research was palm fiber waste, obtained from one of the palm flour manufacturing sites in Klaten. Meanwhile, the chemicals used consisted of NaOH, HCl, $NaClO_2$, glacial acetic acid, methylene blue, and congo red were all bought from PT. Merck Chemicals and Life Sciences, Indonesia.

2.2. Methods

2.2.1. Palm Fiber Preparation

The preparation of palm fiber began with washing the palm fiber using distilled water. After that, the palm fiber was dried. After drying, the palm fiber was cut into small pieces using scissors.

2.2.2. Isolation of Cellulose Nanofibrils

Palm fiber that had been washed and dried was then cut to reduce its size. After that, as much as 3 g of palm fiber cut into small pieces was soaked in 5% NaOH solution at 50°C for four hours. Then, it was rinsed until neutral. Acid hydrolysis was carried out by soaking the palm fiber in a 3.5M HCl solution at 50°C for 24 hours. The fibers were then rinsed to neutral to remove the acid. Next, the fibers were ground to a slurry form and delignified again by soaking them in 5% NaOH solution at 50°C for four hours. It was continued by rinsing until neutral and soaked again in 5M HCl solution for 24 hours. Delignification was then carried out by a bleaching process, using a mixture of $NaClO_2$ and glacial acetic acid in a ratio of 4: 1. After bleaching, the fibers were washed with deionized water until neutral. This method of isolation of cellulose nanofibrils referred to the method already carried out by Chandra et al. [30] with a few modifications.

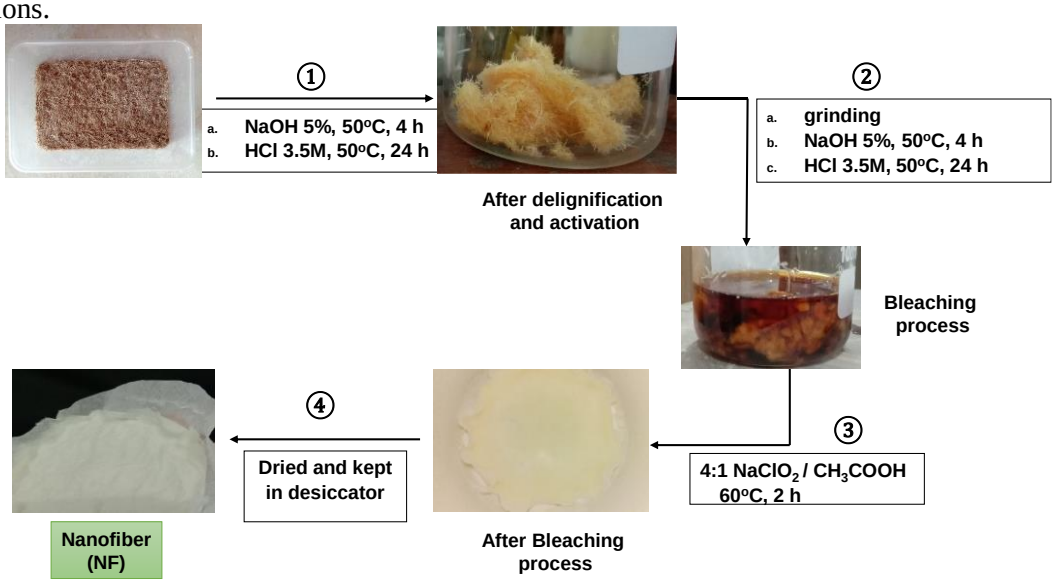

Figure 3. Nanofiber Synthesis Process from Palm Fiber Waste

2.2.3. Nanofiber Coating Method

The nanofiber that had been formed was taken 1 g to be put in a beaker, then 10 mL of $Fe(NO_3)_3$ 3% solution was added, and in another 1 g of nanofiber, 10 mL of 5 $Fe(NO_3)_3$ 5% solution was added. It was stirred until evenly distributed while heated at a temperature of 100°C. After the solution was absorbed into the nanofiber, the nanofiber was oven-dried at 100°C for 30 minutes. After drying, the next step was to calcinate at a temperature of 200°C.

2.2.4. Adsorptivity Test

The adsorption stage started with adding 0.1 g of adsorbent into 100 mL of dye solution with a concentration of 10 ppm. The solution was stirred with temperature variations of 30°C, 40°C, and 50°C for 120 minutes, with intervals of

0, 15, 30, 45, 60, 90, 120 minutes. The solution taken was then filtered before measuring the absorbance. Furthermore, the percentage of adsorbed dye was carried out by processing the absorbance data.

2.2.5. Characterization

The characterization of the synthesized nanofibers was carried out using a Fourier Transformed Infrared (FTIR) spectrometer (Shimadzu IR-Prestige21) to determine the functional groups contained in the nanofiber material. Meanwhile, for material crystallinity analysis, X'pert PRO PANalytical type X-ray diffraction (XRD) was utilized.

3. Results and discussion

3.1. FTIR Analysis

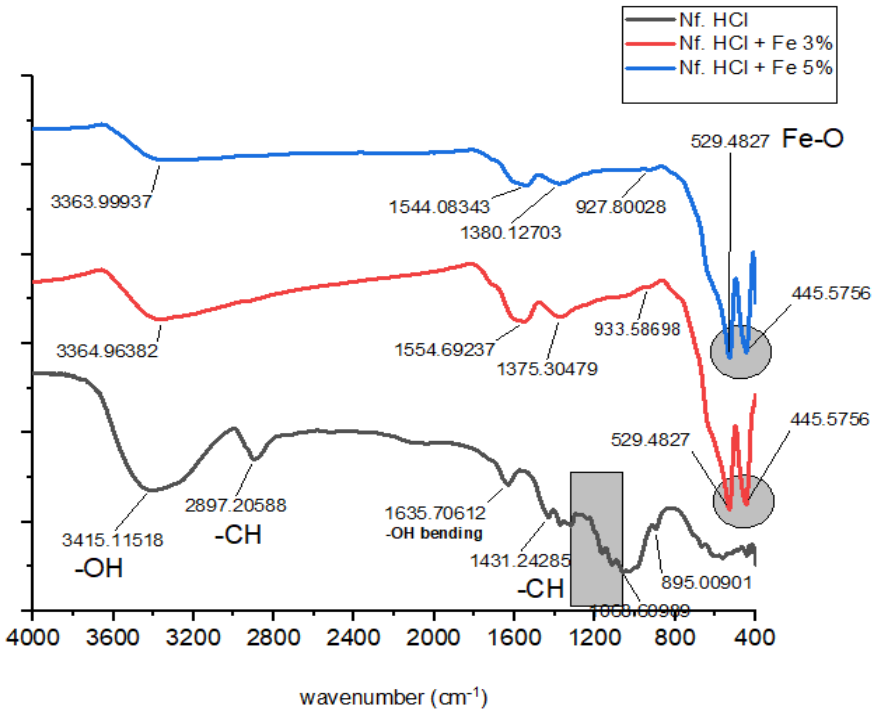

Figure 4. Spectra of Nanofiber and Nanofiber with Iron Oxide (Fe_3O_4) Coating

From the FTIR characterization results in figure 4, it can be seen that all nanofiber samples showed functional groups forming cellulose, namely OH groups, C-O groups, and C-H groups. In the FTIR spectra, the nanofiber samples activated by HCl and did not receive any coating treatment had a peak at 3415.12 cm^{-1}, indicating OH stretching. It is due to the vibration of the hydrogen bonds in the hydroxyl groups of cellulose [31-34]. The peak at 2897.21 cm^{-1} is related to the presence of C−H symmetrical stretching in cellulose [34-36]. In addition, there was also a peak at 1635.71 cm^{-1}, which signifies that the OH bending is related to the hydrophilic characteristics of the fiber [37,38]. The peak at 1431.24 cm^{-1} is related to the C–H deformation vibration of the lignin [32,39]. Furthermore, the presence of peaks in the range of 1112.97-1370.48 cm^{-1} is related to the bending frequency of CH, OH, or CH_2, which specifies deformation bands in cellulose, lignin, and hemicellulose [40-43]. The peak at 1058 cm^{-1} denotes C–O stretching [43,44]. Meanwhile, the peak at 895.97 cm^{-1} is characteristic of β-glycosidic linking glucose units in cellulose. The nanofiber sample, which was activated with HCl and treated with Fe 3% coating, showed an OH group at the peak of 3364.96 cm^{-1}. The wavelength region of 800-1500 cm^{-1} is the unique fingerprint region of cellulose [34]. The peak at 1554.69 cm^{-1} indicates the presence of aromatic ring vibration [32,39]. Besides, the peak at 1375.30 cm^{-1} signifies a C–

H asymmetric deformation [40]. The peak at 933.59 cm^{-1} denotes vibrations from C–O stretching [43]. In addition, the Fe-O functional group indicated by the presence of a peak ranged ≤700 cm^{-1}, namely at the peaks of 529.48 cm^{-1} and 445.58 cm^{-1} [45]. Meanwhile, the nanofiber samples, which were activated with HCl and treated with Fe 5% coating, revealed an OH group at the peak of 3363.99 cm^{-1}. The wavelength region of 800-1500 cm^{-1} is the unique fingerprint region of cellulose [34]. The peak at 1544.08 cm^{-1} means aromatic ring vibration [32,39]. Then, the peak at 1380.13 cm^{-1} implies a C–H asymmetric deformation [40]. The peak at 927.80 cm^{-1} indicates vibrations from C–O stretching [43]. In addition, the Fe-O functional group indicated by the presence of a peak in the range of ≤700 cm^{-1}, namely at the peaks of 529.48 $cm^{-1}$and 445.58 cm^{-1} [45]. Moreover, the absorption band in the range of 3300-3500 cm^{-1} observed in all treatment variations showed the O-H strain vibration of the hydrogen bonding hydroxyl group. It can also be observed that the maximum absorption of the water peak slightly shifted to lower wavenumber (3415.12 cm^{-1} shifted to 3364.96 cm^{-1}), with reduced humidity due to the calcination process at 200ºC for two hours on Fe metal coating treatment. From these results, it can be seen that the iron oxide (Fe_3O_4) coating process on nanofibers has been successfully carried out.

3.2 XRD Analysis

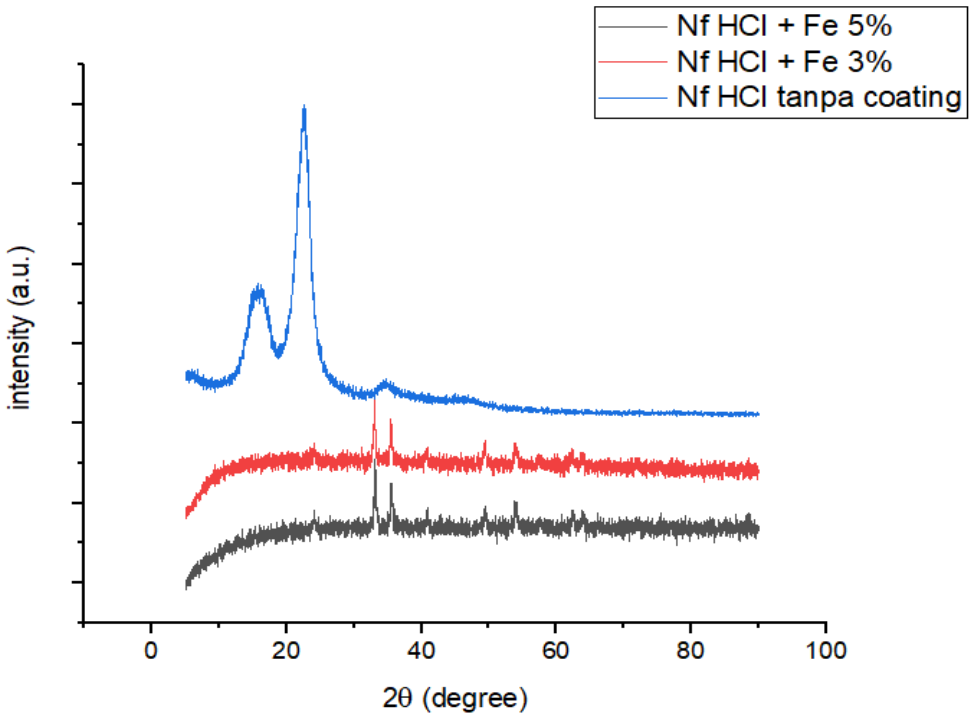

Figure 5. Diffraction of Nanofiber and Nanofiber Coated with Iron Oxide

In figure 5, the blue color spectra displayed the uncoated nanofiber characteristics, which were analyzed using an XRD instrument. Based on figure 5, it can also be seen that this sample produced few peaks with wide and high characteristics. The distribution and peak intensity can be observed in table 1.

Table 1. Distribution and Peak Intensity of Nanofiber Characterization Results without Coating Using XRD

Pos. [°2Th.]	Height [cts]	FWHM Left [°2Th.]	d-spacing [Å]	Rel. Int. [%]
14.8194	304.25	0.8029	5.97796	89.88
16.4423	337.20	0.4015	5.39139	99.62
22.7909	338.50	0.0900	3.89867	100.00

34.4874	52.19	0.5353	2.60068	15.42

Based on table 1, this sample produced four peaks, and three of them had high intensity, namely at position 2θ 14.8194; 16.4423; and 22.7909. Phase analysis of nanofiber samples without coating in this study was based on the nanofibers' characteristics by Yousefi et al. [46].

Based on this reference, WNF was a nanofiber isolated from wood micro-particles (WMP). WMP and WNF showed peaks at 2θ from 15; 16; 22.5 dan 35 associated with cellulose I_β. Among the chemical compounds of wood, cellulose fibers were crystalline and showed peaks on the XRD graph. However, other components, including lignin and hemicellulose, were amorphous polymers with peak widths at 2θ from 18-21° [47]. Qualitatively, the characteristics of the uncoated nanofibers (figure 5, blue spectra) are similar to those of the reference nanofibers. The similarity of the two samples was indicated by the presence of a peak with high intensity and wide at 2θ 22°. In addition, figure 5 red and black color spectra displayed the nanofibers' characteristics with 3% and 5% iron oxide coatings, which were analyzed utilizing XRD instruments. Phase analysis of nanofiber coated with iron oxide in this study was based on the nanofibers' characteristics by Liu et al. [28]. From this reference, XRD characterization of Fe_3O_4/PAN composite NFs samples showed the same diffraction peak of Fe_3O_4 at 2θ, namely at 30.2°, 35.6°,43.4°,57.2°, and 63.0° [28]. By comparing the XRD characterization results of Fe-coated nanofiber samples in this study with references, it can be seen that there were similarities in the characterization results of samples of Nf HCl + Fe 3% and Nf HCl + Fe 5%, namely the presence of strong peaks in each sample of 35.49 and 35.54. The similarity of these peaks indicates the presence of Fe_3O_4 in each nanofiber sample coated with iron oxide (Fe_3O_4). According to the Debye-Scherrer formula, the mean crystal size was estimated based on the expansion of the X-ray diffraction peak according to equation 1 below.

$$D = \frac{K\lambda}{\beta cos\theta} \quad (1)$$

Where D is the crystal size (nm); λ is the wavelength of X-ray radiation (Cu Kα = 0.154060 nm); K is the Scherrer constant (K= 0.9); β is the value of FWHM; and θ is the X-ray diffraction angle. The crystal size of nanofiber samples without coating, nanofiber + Fe 3%, and nanofiber + Fe 5% was 33.888 nm, 36.363 nm, and 31.455 nm, respectively. Meanwhile, the degree of crystallinity of nanofiber samples without coating, nanofiber + Fe 3%, and nanofiber + Fe 5% respectively was 74.933; 34.446; 34.578. From the XRD results in figure 5, it can be observed that the synthesis of nanofibers from palm fiber had been successfully carried out. The mean size of the resulting nanofiber was 33.902 nm. Also, the best degree of crystallinity in the uncoated nanofiber was 74.933.

3.3. ADSORPTION

Congo red and methylene blue adsorption process used nanofiber adsorbents with a mass of 0.1 grams, with variations in contact temperature of 30°C, 40°C, and 50°C and contact time variations of 0, 15, 30, 45, 60, 90, and 120 minutes.

3.3.1. Congo Red

3.3.1.1. Effect of Contact Time

The contact time of adsorbent nanofiber HCl without coating, Nf HCl + Fe 3%, and Nf HCl + Fe 5% to congo red dye waste affected the power of the adsorption process. Determination of the optimum contact time was intended to determine how long the adsorbent could maximally adsorb congo red dye until an equilibrium state was reached between the adsorbed and released dye. In this study, the contact time of the nanofiber adsorbent was varied with HCl without coating, Nf HCl + Fe 3%, and Nf HCl + Fe 5% against congo red dye. Variations in contact time were carried

out at 0, 15, 30, 45, 60, 90, and 120 minutes, with the study results shown in Figure 6. In addition, the adsorption of congo red by HCl nanofiber adsorbent without coating (Fig. 6a) at a temperature of 30ºC increased adsorption capacity from 15 minutes to 120 minutes, so the optimum time at 30ºC was at 120 minutes with an adsorption capacity of 8.58 mg/g. At a temperature of 40ºC, the adsorption capacity increased from the 15th minute to the 90th minute, then decreased to the 120th minute. It can be determined that the optimum time at a temperature of 40ºC was at 90 minutes with an adsorption capacity of 9.71 mg/g. At a temperature of 50ºC, the adsorption capacity increased from the 15th minute to the 90th minute, then decreased to the 120th minute. It can be stated that the optimum time at a temperature of 50ºC was at 90 minutes with an adsorption capacity of 9.71 mg/g.

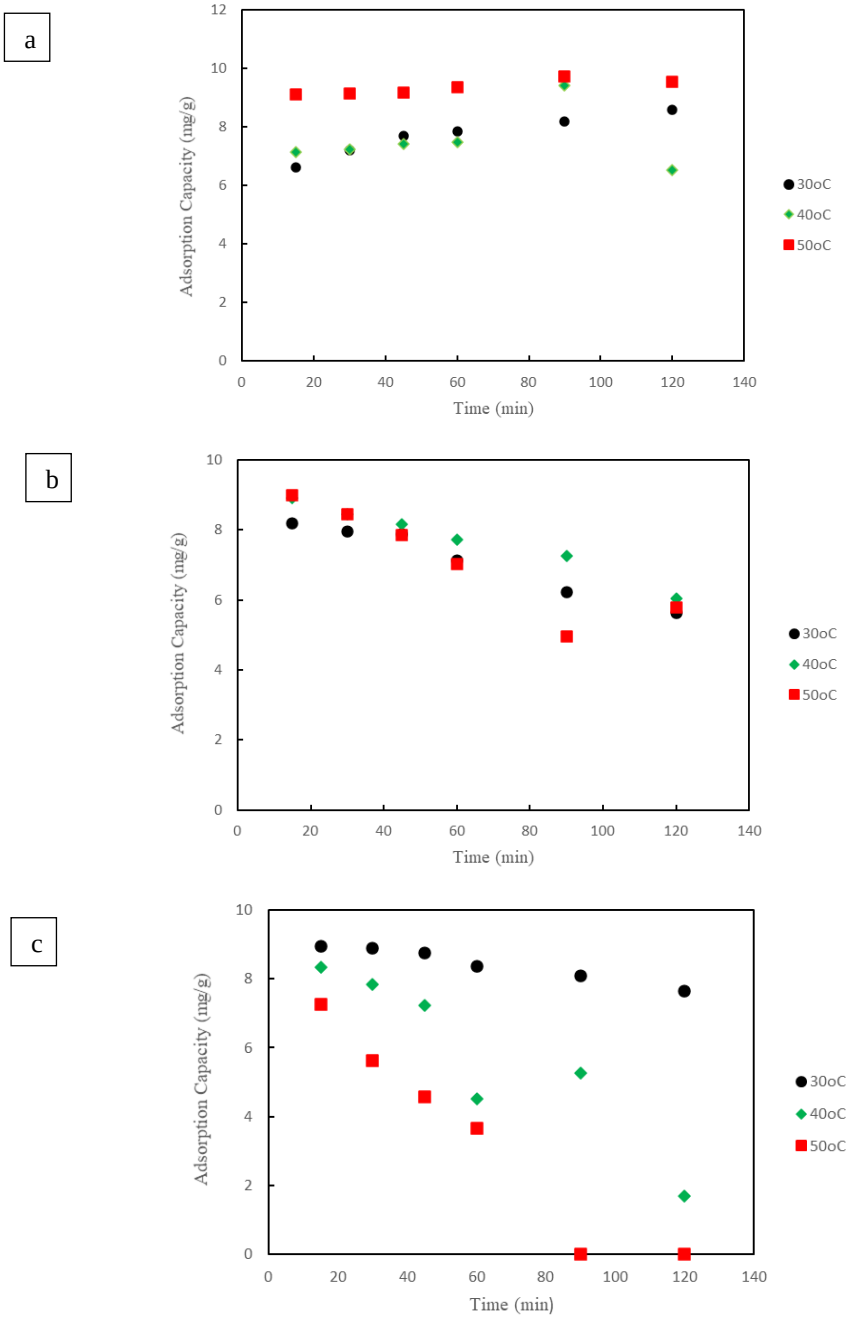

Figure 6. Adsorption capacity (mg/g) of CR using **(a)** Nf HCl without coating, **(b)** Nf HCl + Fe 3%, **(c)** Nf HCl + Fe 5% under various of temperatures

Adsorption of congo red by adsorbent Nf HCl + Fe 3% (Fig. 6b) at a temperature of 30ºC decreased adsorption capacity from 15 to 120 minutes. It was concluded that the optimum time at a temperature of 30ºC was at 15 minutes with an adsorption capacity of 8.18 mg/g. At a temperature of 40ºC, there was also a decrease in adsorption capacity from the 15th minute to the 120th minute. Thus, it can be determined that the optimum time at a temperature of 40ºC was at 15 minutes with an adsorption capacity of 8.92 mg/g. At a temperature of 50ºC, there was a decrease in adsorption capacity from the 15th minute to the 90th minute, then an increase in the 120th minute. It can be specified that the optimum time at a temperature of 50ºC was for 15 minutes with an adsorption capacity of 9.0 mg/g. Furthermore, the adsorption of congo red by the adsorbent Nf HCl + Fe 5% (Fig. 6c) at a temperature of 30ºC increased adsorption capacity from 15 to 30 minutes, then decreased adsorption capacity to 120 minutes. It was inferred that the optimum time at a temperature of 30ºC was at 30 minutes with an adsorption capacity of 8.89 mg/g. At 40ºC, the adsorption capacity also decreased from the 15th minute to the 60th minute, then increased at the 90th minute, and fell again at the 120th minute. It can be determined that the optimum time at a temperature of 40ºC was for 15 minutes with an adsorption capacity of 8.42 mg/g. At a temperature of 50ºC, there was a decrease in adsorption capacity from the 15th minute to the 120th minute, so that it can be stated that the optimum time at a temperature of 50ºC was at 15 minutes with an adsorption capacity of 7.26 mg/g. The decrease in the adsorption capacity of the adsorbent was because the adsorbent used was saturated and exceeded the maximum capacity of the compound that could be adsorbed. Thus, if the contact time is extended, it will not increase the adsorption capacity and tend to decrease the desorption and adsorption capacity [48].

3.3.1.2 Effect of Temperature

One of the factors affecting the adsorption capacity is the solution temperature [49]. In this experiment, the temperature variation of the congo red solution was carried out to determine the temperature's effect on the adsorption process of congo red with nanofiber adsorbents HCl without coating, Nf HCl + Fe 3%, and Nf HCl + Fe 5%. Variations were done at temperatures of 30ºC, 40ºC, and 50ºC. From the three graphs (Fig. 6), it can be observed that when the temperature was increased, the adsorption capacity of the HCl nanofiber without coating increased with the increase in the congo red solution's temperature; likewise, in Nf HCl + Fe 3%. It is because when the temperature is increased, the adsorption will also increase, indicating that the adsorption is endothermic. As the temperature increases (heating), the water molecules will be released due to molecular exchange between the dye molecules and the functional groups of the adsorbent surface [50]. Meanwhile, in the Nf HCl + Fe 5% adsorbent, the adsorption capacity decreased with the increase in the congo red dye solution's temperature. Moreover, the best CR adsorption using Nf HCl adsorbent without coating was at a temperature of 50ºC, while the best CR adsorption using Nf HCl + Fe 3% was at 40ºC, and for CR adsorption using Nf HCl + Fe 5% adsorbent, the best was at 30ºC. If looking at the adsorbents Nf HCl + Fe 3% and Nf HCl + Fe 5%, there was a decrease in adsorption capacity each time the contact time increased. It was probably due to the presence of Fe residue released into the CR solution. In a study conducted by Liu et al. [28], if the acidity is high, H^+ ions will react with Fe_3O_4 and cause the release of Fe ions into the solution.

3.3.2. Methylene Blue

3.3.2.1. Effect of Contact Time

In this study, the contact time of the nanofiber adsorbent was varied with HCl without coating, Nf HCl + Fe 3%, and Nf HCl + Fe 5%, with methylene blue dye at 0, 15, 30, 45, 60, 90, and 120 minutes. It was done to know the optimum time of the methylene blue adsorption process with the three types of adsorbent variations. In the adsorption of methylene blue by HCl nanofiber adsorbent without coating (Fig. 7a) at a temperature of 30ºC, there was a significant

increase in adsorption capacity from 45 to 60 minutes, while at 90 minutes to 120 minutes, there was a slight decrease in adsorption capacity. Thus, the optimum time at 30ºC was 60 minutes with an adsorption capacity of 9.973 mg/g. Meanwhile, at a temperature of 40ºC, there was an increase in adsorption capacity from the 30th minute to the 45th minute, then stuck until the 60th minute, and after 60 minutes, the adsorption capacity decreased. It can be determined that the optimum time at 40ºC was 45 minutes with an adsorption capacity of 9.959 mg/g. At a temperature of 50ºC, there was a decrease from the 15th minute to the 120th minute. Thus, the optimum time at a contact temperature of 50ºC was 15 minutes with an adsorption capacity of 9.539 mg/g. Furthermore, on the adsorption of methylene blue by the adsorbent Nf HCl + Fe 3% (Fig. 7b) at a temperature of 30ºC, there was an increase in adsorption capacity at 30 to 45 minutes, then a decrease in adsorption capacity at the 60th minute to the 120th minute. It was concluded that the optimum time at 30ºC was 45 minutes with an adsorption capacity of 9.924 mg/g. At a temperature of 40ºC, from the 15th minute to the 30th minute, the adsorption capacity remained constant, then decreased from the 45th minute to the 120th minute. Thus, the optimum time at 40ºC was 15 minutes with an adsorption capacity of 9.904 mg/g. At a temperature of 50ºC, there was an increase in adsorption capacity from the 15th minute to the 30th minute; however, at the 45th minute to the 60th minute, there was a decrease in the adsorption capacity. Then, there was a significant increase in the 90th minute and a drastic drop in the 120th minute. Thus, the optimum time at the contact temperature of 50ºC was 90 minutes with an adsorption capacity of 9.698 mg/g.

a

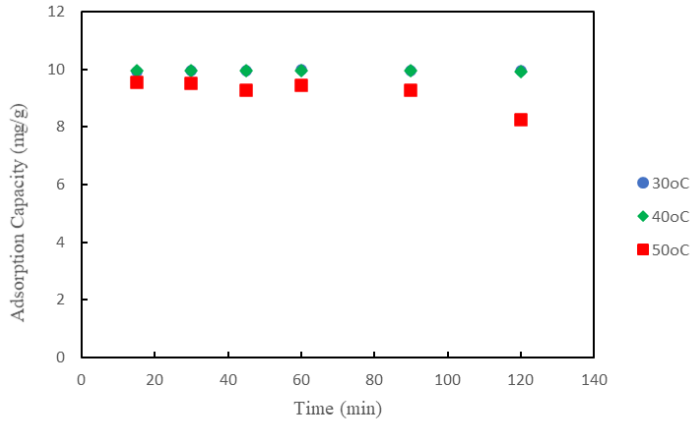

b

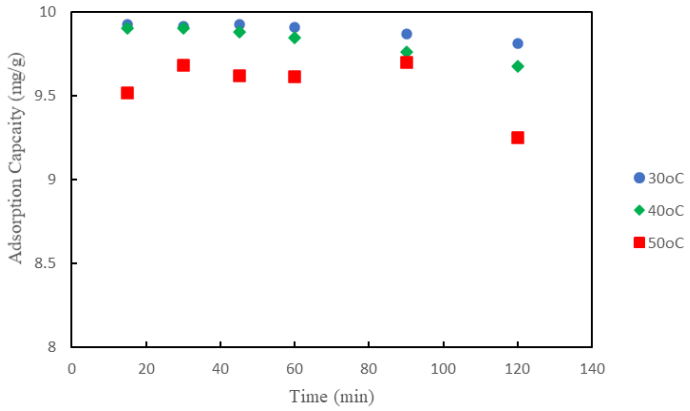

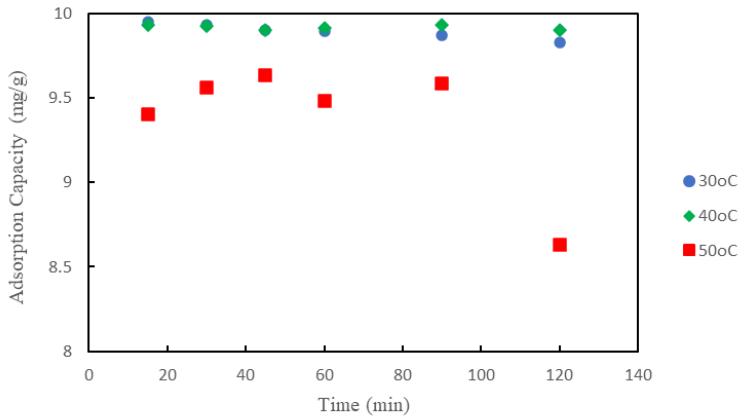

Figure 7. Adsorption capacity (mg/g) of MB using **(a)** Nf HCl without coating, **(b)** Nf HCl + Fe 3%, **(c)** Nf HCl + Fe 5% under various temperatures

Moreover, the adsorption of methylene blue by the adsorbent Nf HCl + Fe 5% (Fig. 7c) at 30ºC decreased the adsorption capacity from the 15th minute to the 120th minute. It could be denoted that the optimum time at 30ºC for this adsorbent was 15 minutes with an adsorption capacity of 9.952 mg/g. At 40ºC, the adsorption capacity also decreased from the 15th minute to the 45th minute, then increased at the 60th minute, and increased significantly again at the 90th minute. However, after that, it decreased in the 120th minute. Thus, the optimum time at 40ºC was 90 minutes with an adsorption capacity of 9.931 mg/g. At a temperature of 50ºC, there was an increase in adsorption capacity from the 15th minute to the 45th minute, and then a drastic decrease occurred at the 120th minute. Thus, the optimum time for the 50ºC contact temperature was 45 minutes with an adsorption capacity of 9.636 mg/g. The decrease in the adsorption capacity of the adsorbent was caused by the adsorbent used was saturated and exceeded the maximum capacity of the compound that could be adsorbed. Therefore, if the contact time is extended, it will not increase the adsorption capacity and tend to decrease the desorption and adsorption capacity [48].

3.3.1.2. Effect of Temperature

One of the factors affecting the adsorption capacity is the solution's temperature [49]. From the three graphs (Fig.7), it can be seen that in HCl nanofibers without coating, Nf HCl + Fe 3%, and Nf HCl + Fe 5% capacity, the adsorption decreased as the methylene blue solution's temperature increased. It denotes that the adsorption process is exothermic. The reduction of the adsorption rate by increasing the temperature may be since the methylene blue dye molecules at higher temperatures have a great ability to be desorbed and pass to the liquid phase [16]. In this case, MB adsorption using adsorbent Nf HCl without coating, Nf HCl + Fe 3%, and Nf HCl + Fe 5% was best at a temperature of 30ºC.

4. Conclusion

Palm fiber waste has been successfully utilized as a nanofiber adsorbent. It was indicated by the presence of functional groups forming cellulose, namely OH groups, C-O groups, and C-H groups in the three synthesis products. In addition, the coating of iron oxide (Fe_3O_4) on nanofibers has also been successful, as revealed by the presence of Fe-O functional groups in the range of ≤700 cm^{-1}, namely at the peaks of 529.48 cm^{-1} and 445.58 cm^{-1}. In addition, the mean size of the resulting nanofiber was 33.902 nm, and the best degree of crystallinity for the nanofiber without coating was 74.933.

Moreover, the addition of an iron oxide (Fe_3O_4) coating could increase the adsorption capacity. However, this adsorbent was more optimal for absorbing basic dyes (MB) than acid dyes (CR). Due to the acidic conditions, it would

allow the release of Fe residues into the solution. It is because if the acidity is high, H^+ ions will react with Fe_3O_4 and cause the release of Fe ions into the solution.

References

[1] Presiden, "Undang - Undang Republik Indonesia Nomor 32 Tahun 2009 tentang Perlindungan dan Pengelolaan Lingkungan Hidup," 2009.

[2] W. A. Wardhana, "Dampak Pencemaran Lingkungan." Andi, Yogyakarta, 2004.

[3] D. Roosmini, M. Septiono, N. Putri, H. Shabrina, I. Salami, and H. Ariesyady, "River Water Pollution Condition in Upper Part of Brantas River and Bengawan Solo River," *IOP Conf.Series Earth Environ. Sci.* 2017, vol. 106, pp. 1–6.

[4] S. W. Kusumastuti, M. Bisri, M. Solichin, T. B. Prayogo, I. Y. Septiariva, and L. M. Limantara, "Water Quality Monitoring and Evaluation in the Bengawan Solo River Region," *Technol. Reports Kansai Univ.* 2020, vol. 62, no. 03, pp. 797–806,

[5] S. R. Couto, "Dye Removal by Immobilised Fungi," *Biotechnol. Adv.* 2009, vol. 27, no. 3, pp. 227–235.

[6] M. Sudha, A. Saranya, G. Selvakumar, and N. Sivakumar, "Microbial Degradation of Azo Dyes: A review," *Int. J. Curr. Microbiol. Appl. Sci.* 2014, vol. 3, no. 2, pp. 670–690.

[7] N. P. Shetti, S. J. Malode, R. S. Malladi, S. L. Nargund, S. S. Shukla, and T. M. Aminabhavi, "Electrochemical Detection and Degradation of Textile Dye Congo Red at Graphene Oxide Modified Electrode," *Microchem. J.* 2019, vol. 146, no. January, pp. 387–392.

[8] R. S. Dewi and S. Lestari, "Dekolorisasi Limbah Batik Tulis Menggunakan Jamur Indigenous Hasil Isolasi Pada Konsentrasi Limbah yang Berbeda," *Molekul*. 2010, vol. 5, no. 2, pp. 75–82.

[9] E. Widjajanti, R. T. P, and M. P. Utomo, "Pola Adsorpsi Zeolit terhadap Pewarna Azo Metil Merah dan Metil Jingga," in *Prosiding Seminar Nasional Penelitian, Pendidikan dan Penerapan MIPA*, 2011, pp. 115–122.

[10] Clark, "Handbook of Textile and Industrial Dyeing." Woodhead Publishing Limited, Britania, 2011.

[11] E. Haque, J. W. Jun, and S. H. Jhung, "Adsorptive Removal of Methyl Orange and Methylene Blue from Aqueous Solution with A Metal-Organic Framework Material, Iron Terephthalate (MOF-235)," *J. Hazard. Mater.* 2011, vol. 185, no. 1, pp. 507–511.

[12] T. An, G. Li, Y. Xiong, X. Zhu, H. Xing, and G. Liu, "Photoelectrochemical Degradation of Methylene Blue with Nano TiO2 Under High Potential Bias," 2001, vol. 4, pp. 101–106.

[13] Q. Xiao, Z. Si, J. Zhang, C. Xiao, Z. Yu, and G. Qiu, "Effects of Samarium Dopant on Photocatalytic Activity of TiO_2 Nanocrystallite for Methylene Blue Degradation," *J. Mater Sci.* 2007, vol. 42, pp. 9194–9199.

[14] V. Ramaswamy, N. B. Jagtap, S. Vijayanand, D. S. Bhange, and P. S. Awati, "Photocatalytic Decomposition of Methylene Blue on Nanocrystalline Titania Prepared by Different Methods," *Mater. Res. Bull.* 2008, vol. 43, pp. 1145–1152.

[15] C. Arora, S. Soni, S. Sahu, J. Mittal, P. Kumar, and P. K. Bajpai, "Iron Based Metal Organic Framework for Efficient Removal of Methylene Blue Dye from Industrial Waste," *J. Mol. Liq.* 2019, vol. 284, pp. 343–352.

[16] M. Y. Nassar, E. A. Abdelrahman, A. A. Aly, and T. Y. Mohamed, "A Facile Synthesis of Mordenite Zeolite Nanostructures for Efficient Bleaching of Crude Soybean Oil and Removal of Methylene Blue Dye from Aqueous Media," *J. Mol. Liq.* 2017, vol. 248, pp. 302–313.

[17] O. Hamdaoui and M. Chiha, "Removal of Methylene Blue from Aqueous Solutions by Wheat Bran," *Acta Chim. Slov.* 2007, vol. 54, pp. 407–418.

[18] Kementerian Lingkungan Hidup, "Peraturan Menteri Lingkungan Hidup Republik Indonesia Nomor 5 Tahun

2014 tentang Baku Mutu Air Limbah,"https://doi.org/10.1177/003231870005200207, 2014.

[19] M. Ahmaruzzaman, “A Review on The Utilization of Fly Ash,” *Prog. Energy Combust. Sci.* 2010, vol. 36, no. 3, pp. 327–363.

[20] M. A. Ashraf, M. J. Maah, and I. Yusoff, “Study of Banana Peel (Musa sapientum) as a Cationic Biosorbent,” *Am. J. Agric. Environ. Sci.* 2010, vol. 8, no. 1, pp. 7–17.

[21] N. Yang, S. Zhu, D. Zhang, and S. Xu, “Synthesis and Properties of Magnetic Fe_3O_4-Activated Carbon Nanocomposite Particles for Dye Removal,” *Mater. Lett.* 2008, vol. 62, pp. 645–647.

[22] Rismang, S. HS, and K. Ramadani, “Sintesis Zeolit dari Abu Layang dengan Metode Hidrotermal dan Uji Adsorptivitas terhadap Logam Timbal (Pb),” *Al-Kimia*. 2017, vol. 5, no. 2, pp. 127–135.

[23] J. Chen, Y. Wei, H. Ji, P. Guo, and D. Wan, “Adsorption of Nitrate and Nitrite from Aqueous Solution by Magnetic Mg/Fe Hydrotalcite,” 2021, vol. 00, no. 0, pp. 1–14.

[24] M. K. Apriliani, T. I. Noor, and M. N. Yusuf, “Analisis Nilai Tambah Agroindustri Tepung Aren (Studi Kasus di Desa Kertaharja Kecamatan Cijeungjing Kabupaten Ciamis),” *J. Ilm. Mhs. Agroinfo Galuh*. 2020, vol. 7, no. 2, pp. 301–309.

[25] J. E. Manatar, J. Pontoh, and M. R. . Runtuwene, “Analisis Kandungan Pati dalam Batang Tanaman Aren (Arenga pinnata),” *J. Ilm. Sains*. 2012, vol. 12, no. 2, pp. 89–92.

[26] M. Firdayati and M. Handajani, “Studi Karakteristik Dasar Limbah Industri Tepung Aren,” *J. Infrastruktur dan Lingkung. Binaan*. 2005, vol. 1, no. 2.

[27] Wijoyo, A. Nurhidayat, and C. Purnomo, “Kajian Pengaruh Fraksi Volume Serat Akibat Perlakuan Alkali terhadap Ketangguhan Impak Komposit Limbah Serat Aren-Polyester,” 2011, vol. 1, no. 2.

[28] Q. Liu, L. Bin Zhong, Q. B. Zhao, C. Frear, and Y. M. Zheng, “Synthesis of Fe_3O_4/Polyacrylonitrile Composite Electrospun Nanofiber Mat for Effective Adsorption of Tetracycline,” *ACS Appl. Mater. Interfaces*. 2015, vol. 7, no. 27, pp. 14573–14583.

[29] A. Karamipour, P. Khadiv Parsi, P. Zahedi, and S. M. A. Moosavian, “Using Fe_3O_4-Coated Nanofibers Based on Cellulose Acetate/Chitosan for Adsorption of Cr(VI), Ni(II) and Phenol from Aqueous Solutions,” *Int. J. Biol. Macromol.* 2020, vol. 154, no. Vi, pp. 1132–1139.

[30] J. C. C. S, N. George, and S. K. Narayanankutty, “Isolation and Characterization of Cellulose Nanofibrils from Arecanut Husk Fibre,” *Carbohydr. Polym.* 2016, vol. 142, pp. 158–166.

[31] J. F. Mano, D. Koniarova, and R. L. Reis, “Thermal Properties of Thermoplastic Starch/Synthetic Polymer Blends with Potential Biomedical Applicability,” *J. Mater. Sci. Mater. Med.* 2003, vol. 14, pp. 127–135.

[32] M. Sain and S. Panthapulakkal, “Bioprocess Preparation of Wheat Straw Fibers and Their Characterization,” *Ind. Crops Prod.* 2006, vol. 23, pp. 1–8.

[33] S. Elanthikkal, U. Gopalakrishnapanicker, S. Varghese, and J. T. Guthrie, “Cellulose Microfibres Produced from Banana Plant Wastes: Isolation and Characterization,” *Carbohydr. Polym.* 2010, vol. 80, no. 3, pp. 852–859.

[34] D. Chen, D. Lawton, M. R. Thompson, and Q. Liu, “Biocomposites Reinforced with Cellulose Nanocrystals Derived from Potato Peel Waste,” *Carbohydr. Polym.* 2012, vol. 90, no. 1, pp. 709–716.

[35] H. P. S. A. Khalil, H. Ismail, H. D. Rozman, and M. N. Ahmad, “The Effect of Acetylation on Interfacial Shear Strength between Plant Fibres and Various Matrices,” *Eur. Polym. J.* 2001, vol. 37, pp. 1037–1045.

[36] P. R. Sharma, R. Joshi, S. K. Sharma, and B. S. Hsiao, “A Simple Approach to Prepare Carboxycellulose Nanofibers from Untreated Biomass,” *Biomacromolecules*. 2017, vol. 18, pp. 2333–2342.

[37] J. Lojewska, P. Miskowiec, T. Lojewski, and L. M. Proniewicz, “Cellulose Oxidative and Hydrolytic

Degradation: In Situ FTIR Approach," *Polym. Degrad. Stab.* 2005, vol. 88, pp. 512–520.

[38] M. Le Troëdec, C. S. Peyratout, A. Smith, and T. Chotard, "Influence of Various Chemical Treatments on the Interactions between Hemp Fibres and a Lime Matrix," *J. Eur. Ceram. Soc.* 2009, vol. 29, pp. 1861–1868.

[39] R. C. Sun, J. Tomkinson, Y. X. Wang, and B. Xiao, "Physico-Chemical and Structural Characterization of Hemicelluloses from Wheat Straw by Alkaline Peroxide Extraction," *Polymer (Guildf).* 2000, vol. 41, pp. 2647–2656.

[40] X. F. Sun, F. Xu, R. C. Sun, P. Fowler, and M. S. Baird, "Characteristics of Degraded Cellulose Obtained from Steam-Exploded Wheat Straw," *Carbohydr. Res.* 2005, vol. 340, pp. 97–106.

[41] M. K. Nacos *et al.*, "Kenaf Xylan – A Source of Biologically Active Acidic Oligosaccharides," *Carbohydr. Polym.* 2006, vol. 66, pp. 126–134.

[42] M. Le Troedec *et al.*, "Influence of Various Chemical Treatments on The Composition and Structure of Hemp Fibres," *Compos. Part A Appl. Sci. Manuf.* 2008, vol. 39, pp. 514–522.

[43] Y. Chen, C. Liu, P. R. Chang, X. Cao, and D. P. Anderson, "Bionanocomposites Based on Pea Starch and Cellulose Nanowhiskers Hydrolyzed from Pea Hull Fibre: Effect of Hydrolysis Time," *Carbohydr. Polym.* 2009, vol. 76, no. 4, pp. 607–615.

[44] A. Alemdar and M. Sain, "Biocomposites from Wheat Straw Nanofibers: Morphology, Thermal and Mechanical Properties," 2008, vol. 68, pp. 557–565.

[45] S. K. Panda *et al.*, *Magnetite Nanoparticles as Sorbents for Dye Removal: A Review*. Springer International Publishing, 2021.

[46] H. Yousefi, V. Azari, and A. Khazaeian, "Direct Mechanical Production of Wood Nanofibers from Raw Wood Microparticles with No Chemical Treatment," *Ind. Crops Prod.* 2018, vol. 115, no. May 2018, pp. 26–31.

[47] S. H. Saleh and A. A. Aziz, "Polymer Characterization of Cellulose and Hemicellulose," *Polym. Sci. Res. Adv. Pract. Appl. Educ. Asp.* 2016, pp. 404–411.

[48] L. Hadayani, I. Riwayati, and R. Ratnani, "Adsorpsi Pewarna Metilen Biru Menggunakan Senyawa Xanthat Pulpa Kopi," *J. Momentum UNWAHAS*. 2015, vol. 11, no. 1, p. 114174.

[49] G. D. Değermenci, N. Değermenci, V. Ayvaoğlu, E. Durmaz, D. Çakır, and E. Akan, "Adsorption of Reactive Dyes on Lignocellulosic Waste; Characterization, Equilibrium, Kinetic and Thermodynamic Studies," *J. Clean. Prod.* 2019, vol. 225, pp. 1220–1229.

[50] A. Banaei, S. Samadi, S. Karimi, H. Vojoudi, E. Pourbasheer, and A. Badiei, "Synthesis of Silica Gel Modified with 2,2′-(hexane-1,6-diylbis(oxy)) dibenzaldehyde as A New Adsorbent for the Removal of Reactive Yellow 84 and Reactive Blue 19 Dyes from Aqueous Solutions: Equilibrium and Thermodynamic Studies," *Powder Technol.* 2017, vol. 319, pp. 60–70.